LAWRENCE
LIVERMORE
NATIONAL
LABORATORY

UCRL-TR-202407

Electromagnetic Imaging of CO2 Sequestration at an Enhanced-Oil-Recovery Site

B. Kirkendall, J. Roberts

February 18, 2004

This work was performed under the auspices of the U.S. Department of Energy by University of California, Lawrence Livermore National Laboratory under Contract W-7405-Eng-48.

Abstract

The two year LDRD-ER-089 project *Electromagnetic Imaging of CO_2 Sequestration at an Enhanced-Oil-Recovery Site* used a dual track approach to imaging and interpreting the effectiveness and migration of CO_2 injection at an enhanced oil recovery site. Both field data and laboratory data were used together to aid in the interpretation and understanding of CO_2 flow in a heavily fracture enhanced oil recovery site. In particular, project highlights include;

- The development of a low-noise digital field system to measure the EM induction response to CO_2 in a variety of field conditions. Central to this system is a low-noise induction receiver antenna that can measure the low-energy response of the CO_2. This system has consistently measured a shallow pseudo-miscible CO_2 flood at source frequencies between 2.0 kHz and 10 kHz. In addition, the existing and added oil and brine in the formation have also been characterized.

- Comparisons of cross-well images with induction logs acquired before drilling suggest the EM induction resolution for CO_2 imaging is equivalent with applications to waterflood imaging completed at LLNL.

- The development and use of laboratory equipment to conduct fluid and gas time-lapsed injection studies of core samples using fluids acquired in the field. Measurements of the resistivity during this injection process and the ability to make instantaneous measurements of the frequency response provide a unique dataset for interpretation.

- The development of an optimum finite difference grid spacing that allows for stable inversions at different frequencies.

- The use of time-lapse field images to show the change of electrical conductivity in the field scales to the laboratory results. Using this result, we can approximate an interpretation of field images based on the rate-of-change of the laboratory results.

- The application of Q-domain processing is not applicable at this site due to high ground conductivity. Q-domain processing requires three decades of frequency to properly spline a waveform. However, this site is limited to two decades of frequency because the high ground conductivity precludes the highest frequency measurement.

- Using these results, we are currently prepared to study other CO_2 sites at greater depths where the CO_2 and existing petroleum components are miscible.

- Journal paper being prepared for submission to Geophysical Journal International

Introduction

Electromagnetic (EM) methods are highly sensitive to the amount, state, and composition of subsurface fluids, while seismic methods provide information concerning subsurface structure. Borehole EM techniques can be applied to the tasks of characterizing subsurface resources and monitoring production and resource recovery processes in the oil field because of the subsurface fluid information provided by EM methods. These techniques have numerous applications including the focus of this paper, enhanced oil recovery (EOR). The technique of cross-borehole EM induction uses kilohertz-frequency EM fields to image the electrical conductivity structure in the plane intersecting two boreholes. Recent efforts to study and increase borehole EM field and processing resolution (Berryman, 2000), borehole EM inversion algorithm efficiency, and borehole ambient noise sources have resulted in advances in producing consistent cross-borehole EM tomographic images. However, the interpretation of these tomographic EM images remains an undeveloped science.

Using cross-borehole EM induction imaging, we improve interpretation techniques by incorporating petrophysical analysis from core samples, formation fluids, and injection fluids obtained from the site. We account for resistivity values in samples saturated with both formation fluid and injection fluid, determine the volume of oil moved through the sample during brine injection, and provide information on resistivity as a function of injection time for the core samples. We develop a qualitative interpretation approach that uses field images and petrophysical results from laboratory analyses to assign accurate conductivity values for inversion images and to gain a clearer picture of the extent and effectiveness of EOR using water injection.

The site under investigation, defined as a heavy oil reservoir producing with an API index of 17, consists predominantly of high-porosity and extremely low-permeability diatomaceous deposits. EOR in the area has proven somewhat ineffective because fracture-induced injection flow dominates matrix flow. The ability to rapidly image the flow of water injection is therefore crucial to optimizing EOR and understanding the subsurface system. The purpose of this paper is to report field and laboratory results for an active, well-characterized EOR site and to demonstrate interpretations which include analysis and consideration of physical properties determined by borehole and laboratory methods help obtain more in-depth understanding of injection and EOR processes. These methods can be applied to an arbitrary site.

Lawrence Livermore National Laboratory was involved in a 2 year study using time-lapse multiple frequency electromagnetic (EM) characterization at a carbon dioxide (CO_2) sequestration enhanced oil recovery (EOR) site in California operated by Chevron-

Texaco Production Division (Lost Hills, California) and was funded by a two year LDRD-ER (ERD-089). The impetus for this research project was to continue to develop the ability to image subsurface injected CO_2 during EOR processes while simultaneously discriminating between pre-existing petroleum and water deposits. We proposed to combine laboratory and field methods to image a pilot CO_2 sequestration EOR site using the cross-borehole EM technique, improve the inversion process in CO_2 studies by coupling results with petrophysical laboratory measurements, and focus on new supercritical CO_2 interpretation techniques. Field and laboratory results were the main sources of information on subsurface CO_2 detection, CO_2 migration tracking, and displacement of petroleum and water over time. This project directly addressed national energy issues in two ways: 1) the development of field and laboratory techniques to improve in-situ analysis of oil and gas enhanced recovery operations and 2) this study provided a tool for in-situ analysis of CO_2 sequestration, an international technical issue of growing importance. The exit strategy for this proposal was follow-on funding with a NGOTP project at Elk Hills Petroleum Reserve that was not funded due to decreases in the NGOTP budget for the foreseeable future. The results of this project, however, demonstrate an ability to image and interpret CO_2 movement in the subsurface using combined laboratory and field approaches.

Site Background

Previously a waterflood site, the CO_2 injection location (Figure 1) has typically produced a lower petroleum yield than expected during primary and secondary recovery operations. While CO_2 injection for EOR provides the advantage of higher production yields and viscosity reduction in heavy oil, it has the disadvantage of increased cost. Sequestration of industrially produced CO_2 can significantly offset such cost increases. LLNL and Chevron-Texaco were, therefore, interested in a long-term study into the feasibility of CO_2 injection for the purposes of carbon sequestration and subsurface petroleum mobilization with the eventual possibility of running a gas pipeline to injection boreholes if such processes prove economically viable.

In June, 2000, two fiberglass cased observation boreholes were drilled by Chevron, core and fluid samples were made available to LLNL, and, because of the highly corrosive CO_2 environment, two of the four pre-existing injection boreholes were also redrilled and electrically characterized. Chevron began injecting CO_2 into the mature waterflood site in December 2000 and reached full injection pressure in February 2001. LLNL began using this site in FY2001 with an understanding with Chevron Texaco that any results of fluid and CO_2 movement would be presented to Chevron-Texaco in return for full access to the sites. This opportunity to image a carbon sequestration EOR site was unique because it provided a highly controlled and characterized subsurface through a pre-injection deployment to acquire a baseline image and unrestricted access to the observation boreholes. A pre-sequestration baseline survey was acquired in August, 2000 and subsequent surveys were acquired during active CO_2 sequestration in April, 2001 and October, 2001, July, 2002.

CO_2 injection ended unexpectedly in December, 2002 due to problems with excessive sand being produced in the pumping wells. The cause of the loose sand is either attributed to the presence of the CO_2 or the highly fractured nature of the subsurface. In February 2003, one of the observations wells ruptured while being used by another logging company. This observation well began producing oil at the rate of 8 bbl per day and Chevron-Texaco made the decision to deactivate the well. It was therefore not possible to acquire post- CO_2 injection images at the site as was originally intended.

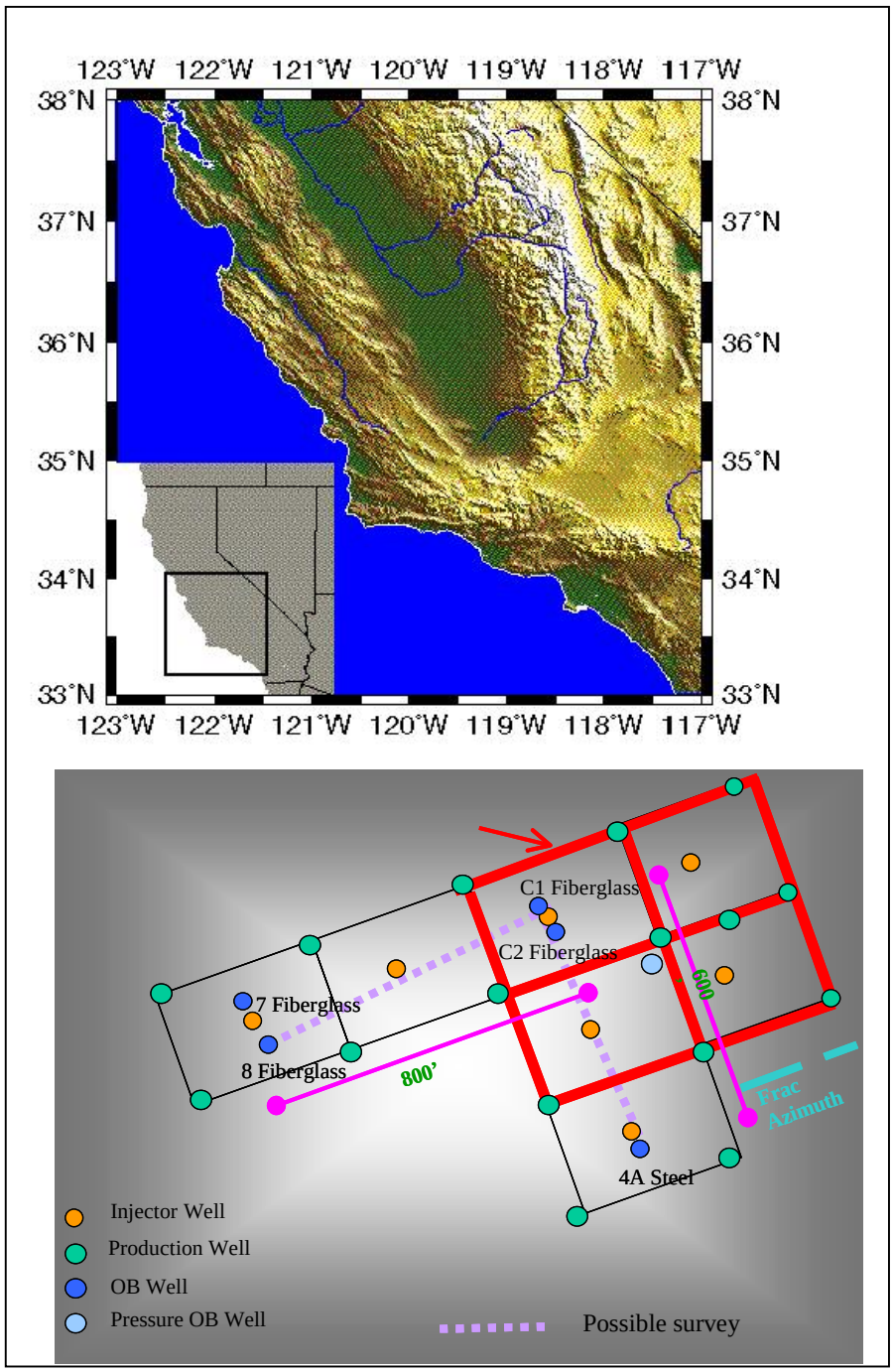

Figure 1: Upper map in GMT format (http://gmt.soest.hawaii.edu/) showing the location of the heavy oil recovery site used for LDRD-ER-089 research. Lower planview shows the relative locations of the wells in the area including the two observation wells used by LLNL C1 and C2 which are fiberglass and nonconductive and thus allow low frequency EM studies.

Geologic Site Parameters

The Lost Hills oil field is located along the crest of the Lost Hills anticline in California's San Joaquin Valley. This anticline is the southernmost segment of a northwest-trending segmented antiform that includes the Kettleman Hills anticlines and the Coalinga anticline to the north. It is located on the western margin of the San Joaquin Basin and roughly parallels the trace of the San Andreas fault zone 32 km to the west (Figure 1). The San Andreas fault system is thought to be the dominant control for structure in the western San Joaquin Valley oil fields (Miller et al., 1990).

The Lost Hills oil field was discovered in 1911, but substantial production did not occur until the 1960's. Presently, oil is produced via steam and waterflooding from a series of stacked oil sands ranging from the Miocene Monterey shales and diatomites to the Pleistocene Tulare sands. The Tulare Formation records the Pleistocene history of basin filling in the present-day San Joaquin valley. It is the first non-marine deposit to be preserved, unconformably overlying the marine Pliocene/Miocene Etchegoin Formation. The unconformity at the underlying units contains numerous normal faults while the Tulare is largely unfaulted and has apparently filled in the older faulted eroded surface.

Permeabilities range from a few hundred millidarcies in muddy sands to between 100 and 3000 millidarcies in the clean sands. For the samples used in this study, the permeabilities range between 1.3 and 39.4 millidarcies and the total porosity ranges from 44 to 63%. Oil saturations range between 35 and 75% with a weighted average of 65% (Wilt et al., 1995) and the oil ranges from 10 to 17 API index.

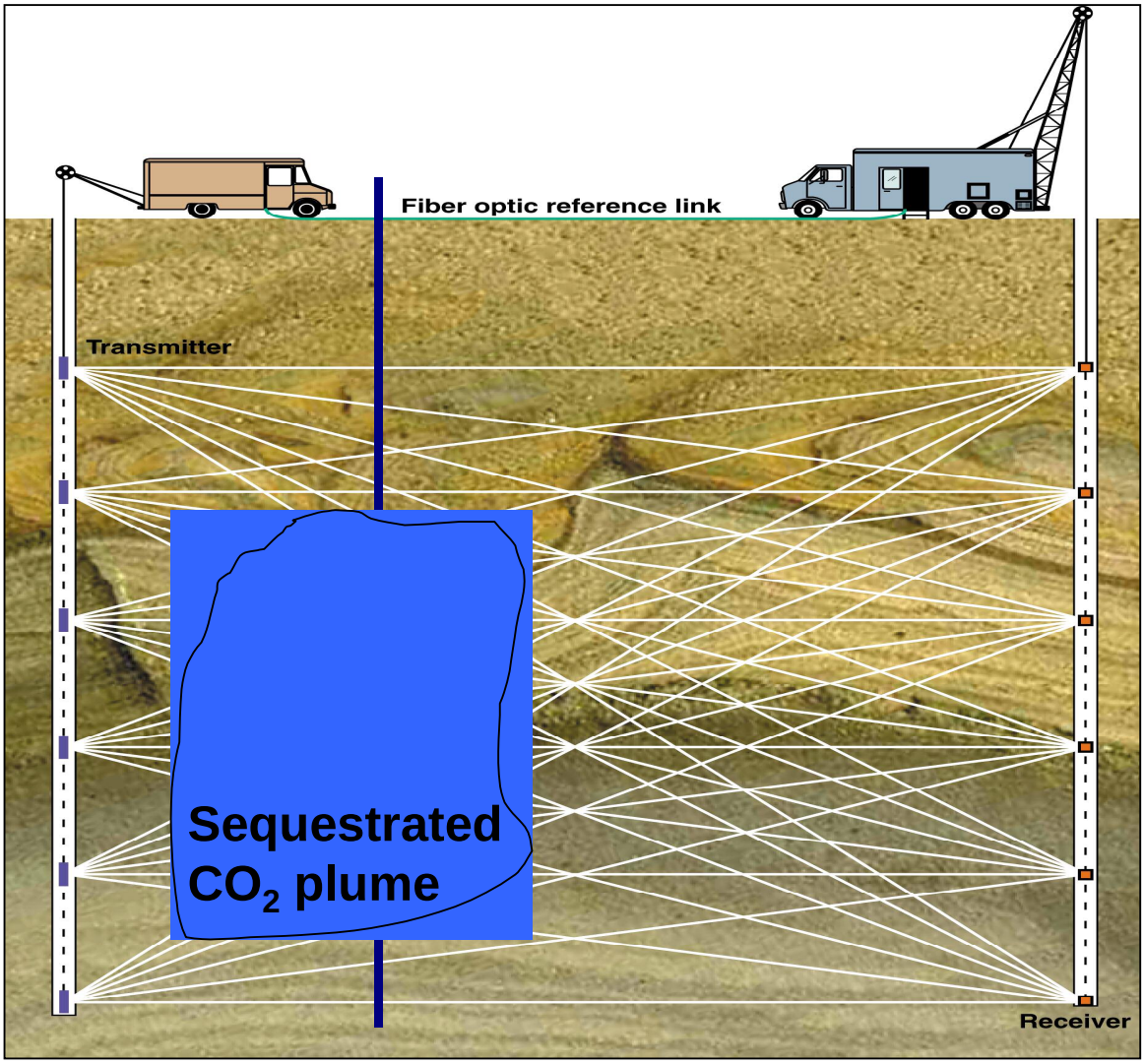

Figure 2: Using crosswell techniques similar to tomography, we image around the injected CO_2 and watch the change over time. Imaging CO_2 is difficult using EM because the contrast with the background oil is small. We can use resolution-enhancing techniques, however, such as multiple frequency image stacking, low noise antennas, and laboratory data to help enhance the subtle differences between the CO_2 and oil. The benefits are strong: a high resolution and cost effective means of imaging CO_2 for sequestration and EOR operations in a variety of geologic conditions.

Laboratory Experimental Techniques

A four-terminal pair, two-electrode lead configuration was used to measure the complex impedance as a function of frequency. Data were taken with an HP 4284A LCR meter. All instruments are high-input impedance devices that measure impedance magnitude $|Z|$, phase angle ϕ, resistance R, and capacitance C. The error of measurement varies according to frequency and resistance, but is generally less than 1% up to 100 kΩ, and within 5% at the highest impedance limits (>100 MΩ). The system was periodically checked for accuracy using a set of 1% tolerance resistors and capacitors and was found to yield consistent values. A photograph of the front end of this apparatus can be seen in Figure 3.

We measured the electrical properties of rocks from the site at conditions of full liquid saturation with oil and as they are invaded with liquid and gaseous (or supercritical) CO_2, and brine. Measurements were performed at temperatures and pressures identical to field conditions in a specially constructed device specifically aimed at these types of measurements. The system consists of an externally heated fluid pressure vessel capable of confining pressures up to 15 MPa and temperatures up to 300°C. Pressure is controlled by three different pressure systems—one each for confining pressure and upstream and downstream pore pressure control. Electrical measurements were performed using two systems, a Hewlett-Packard HP4284A impedance bridge and a Solartron 1260 impedance analyzer. The HP4284A is used to monitor the sample at specific frequencies during periods of heating, pressure changes, and fluid injection. The impedance analyzer is used to make broadband measurements (10^{-3} to 10^{6} Hz) during periods when the sample is at stable experimental conditions. The device and measurement methodology has been tested on oil-filled diatomite samples from the Lost Hills that were injected with brine during EOR. These preliminary measurements showed some unexpected electrical behavior, resistivity increasing during brine injection, that helped interpret the Chevron well-logs and the LLNL crosswell inversions (Kirkendall and Roberts, 2004).

Temperature was measured with type T thermocouples with an accuracy of ±2°C. Comparison of the thermocouples with calibrated standards indicated higher precision, on the order of ±0.2°C. Data collection was automated by use of a scanning unit and microcomputer. Pressures were measured using transducers with an accuracy of ±0.05 MPa. Confining pressure was typically held to 3.5 MPa, but ranged from 0.1 to 5.5 MPa during the course of the experiment. Pore pressure ranged from 0.1 MPa to 3.7 MPa, but was typically half that of the confining pressure.

The cylindrical sample having dimensions of 2.5 cm diameter and ~2.0 cm length is placed between two perforated Pt electrodes and Hastaloy endcaps. The endcaps have channels for the introduction of fluid and are welded to high pressure capillary tubing that serves as pore pressure lines. The entire assembly is jacketed with a high temperature polymer and the entire assembly is held together in a stainless steel frame to prevent separation of the electrodes from the sample during boiling events. Electrodes, thermocouples and pressure lines exit the pressure vessel through insulated conical fittings.

Samples were cut from teflon jacketed core plugs provided by Chevron. Samples were jacketed, assembled and placed in the experimental device. Confining pressure was increased to approximately 3.4 MPa followed by heating to the approximate temperature of the in situ sample according to borehole logs, between 30 and 50°C. After the experiment the resistivity data were corrected to the precise temperature of the sample's depth using the measured temperature dependence. Once the sample was finished heating and reached a stable resistivity, crude oil produced from the Lost Hills oil field was flowed through the sample. The electrical resistivity of the oil is greater than 7.7 x 10^4 ohm-m (σ = 0.013 μS/cm). The pore pressure required to force oil through the samples varied between approximately 1.0 and 2.8 MPa, depending on sample permeability. Oil was flowed through the sample until no water was observed in the exit fluid that was collected and the resistivity again reached a stable value. This value is assumed to be the oil-saturated resistivity from prior research, along with other sample parameters including temperature, reported permeability, brine saturated resistivity, and the resistivity ratio.

Once oil-saturated, the pore fluid was changed to a NaCl brine of resistivity 0.28 ohm-m (σ = 3.57 S/m). This solution was utilized because it has the same electrical conductivity as the brine, but was a cleaner solution that would not damage or contaminate the pumping system and reservoirs. The resistivity was continuously monitored while the brine pushed oil out of the sample. Both fluids were collected permitting estimates of the total volume of fluid flowed. The experiment was ended when the resistivity reached a stable, non-changing value.

This experimental method was adapted for the CO_2 injection process. A well-characterized water- or oil-saturated sample is placed in the vessel for electrical measurements at the temperature of the formation (~38-45 C) and a variety of confining and pore pressures. Supercritical CO_2 is then forced into the sample and the electrical properties monitored as the liquid water or oil is pushed out. This is easily accomplished

at room temperature, as the critical pressure for CO_2 at 18°C is ~7.3 kPa (CRC, 1983), and are well within the operating parameters of the device. Changes in the electrical properties are noted during the phase change. The electrical properties are monitored for a period of time as the sample is held at static conditions to determine if there are long-term effects due to chemical changes. It is important that there is some knowledge of surface conduction mechanisms in the rocks so that any changes in electrical properties because of different surface tensions and wetting behavior can be discerned and understood. The contribution to total conduction due to surface conduction mechanisms can sometimes be gained by performing measurements as a function of effective pressure and by examining the frequency-dependence of conduction.

Laboratory Experimental Results

Results from have identified several key properties of these reservoir rocks. Figure 4 shows the resistivity of a sample as a function of time as the sample is oil, CO_2 and brine saturated. The resistivity changes gradually as CO_2 is injected, but drops quickly when brine enters the sample. This result indicates that it may be possible to discriminate between insulating fluids as well as brine. Additional measurements of frequency dependent electrical properties indicate that oil and CO_2 have a distinctly different frequency response than the brine-saturated samples (Figure 9b). This will also assist in the discrimination of pore fluids based on field surveys. A strong surface conduction mechanism has been found to be present in all rocks studied thus far. This mechanism has been observed in plots of resistivity as a function of effective pressure, where the resistivity shows a negative dependence on effective pressure (Kirkendall and Roberts, 2004). A key factor is that this pressure dependence changes distinctly when CO_2 has passed through the sample. Thus, the injection of CO_2 in the field could have an effect on the observed resistivity in addition to the displacement of other fluids.

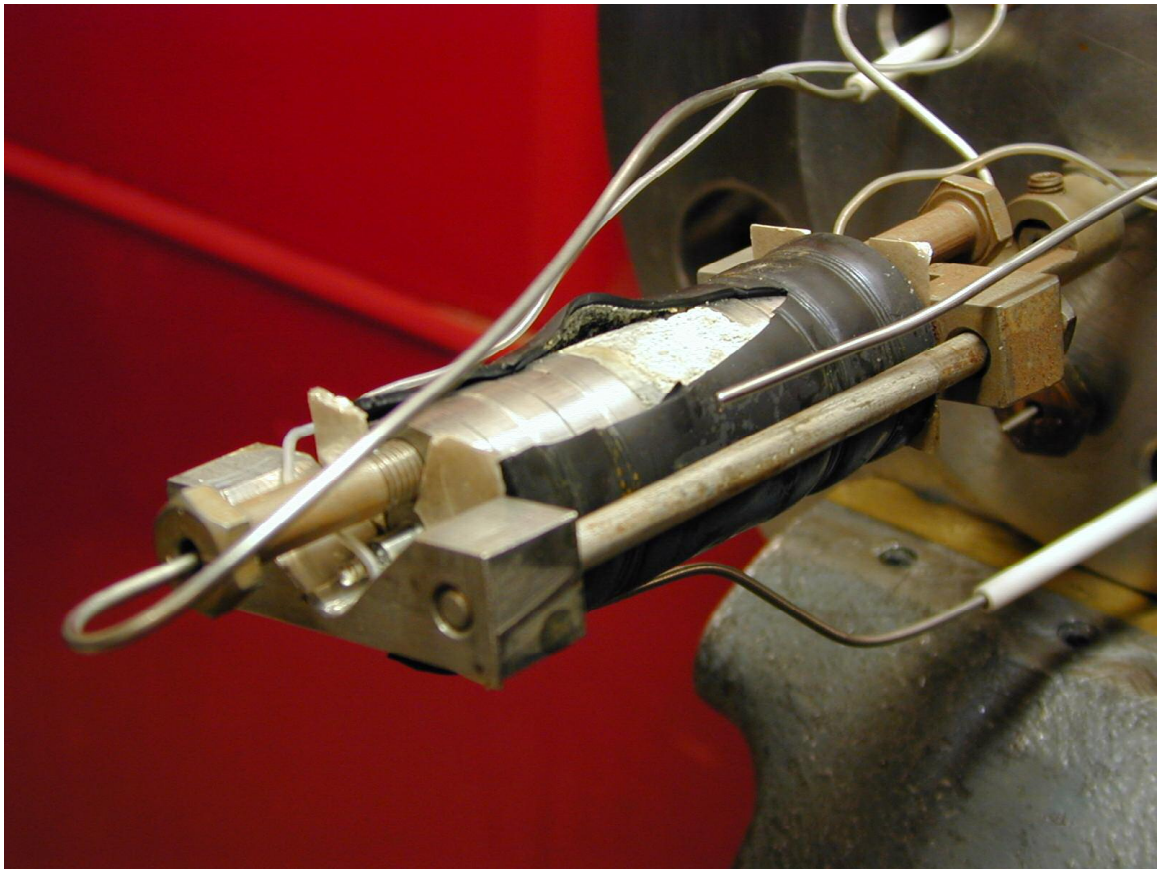

Figure 3: Picture of the measurement apparatus with the shrinkwrap sheathing separated. The core can be seen as well as the vise holder that simulates reservoir conditions. In addition, the tubes leading into and out of the core can hold brine, petroleum, or CO_2 in a supercritical phase. Between the vise and core sample are platinum electrodes that apply and measure the voltage difference to calculate the electrical resistivity as a function of time. This apparatus has also been adapted to accept a network analyzer, which can give a broadband frequency response of the sample at an instantaneous time.

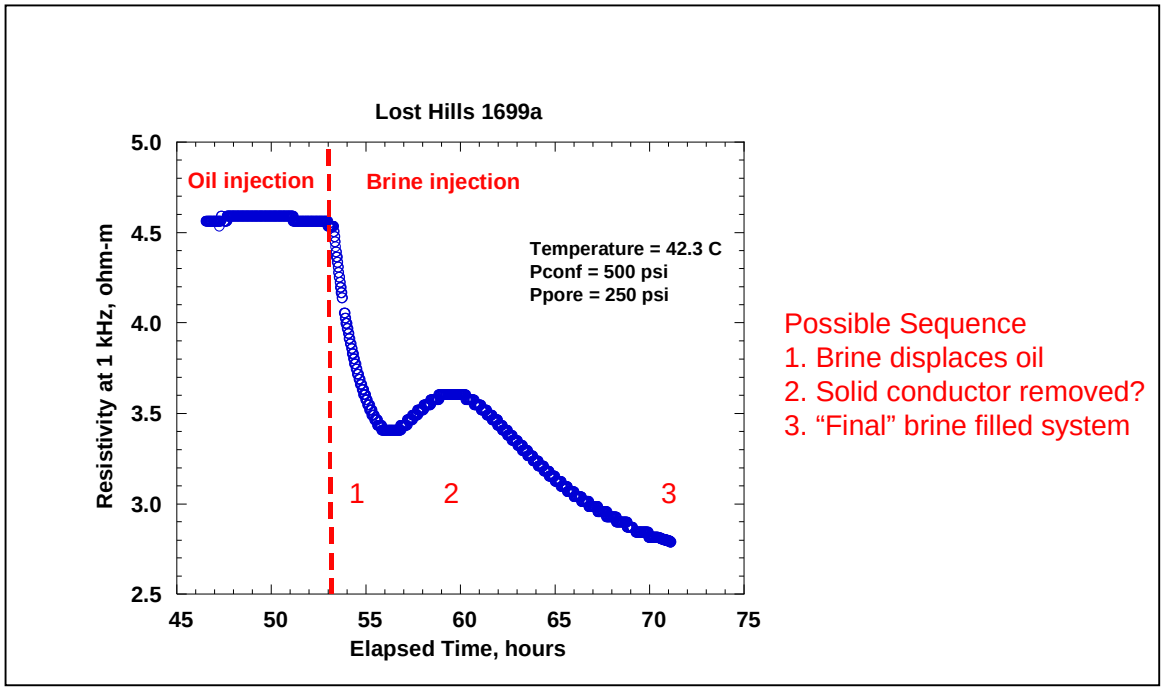

Figure 4: Electrical resistivity of oil-saturated diatomite from Lost Hills, CA during water injection. Resistivity of some sample increases temporarily during the brine injection process. This helps explain the relative lack of low resistivity in parts of the well-logs expected for brine saturated rocks.

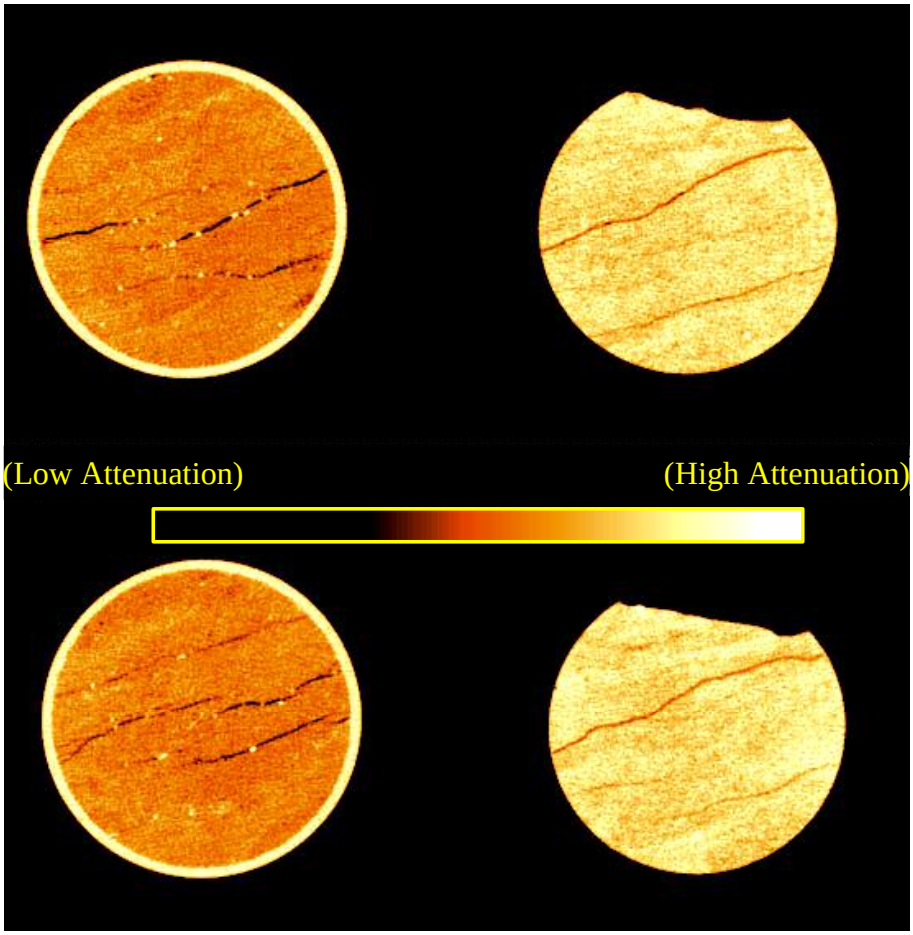

Figure 5: X-ray imaging permits evaluation of fracture flow, fingering, and sweep efficiency. The upper and lower core samples represent two different slices in the core sample. The left, reddish, images were acquired before CO_2 injection. A solid conductor can be seen as white specks in the fractures within the rock matrix. After CO_2 and brine injection, the samples on the right hand side show increased attenuation due to the increased conductivity of the brine fluid and the surface conductor appears to be removed. This surface conductor is likely dissolved into the CO_2 and / or brine solution and would act to increase the electrical conductivity for a short time instead of lower the electrical conductivity as would be expected.

We completed the CO_2 injection experiments with the core samples that include resistivity versus time and pore saturating fluid and broad-bandwidth frequency responses at specific injection times in February 2003. These data sets include a long-term experiment to monitor the changing resistivity while the sample is saturated with CO_2. Additional x-ray imaging of core samples were performed in FY2002 to assess the sweep efficiency of CO_2. Geochemical work was performed to develop a module to calculate the electrical conductivity of fluids based on temperature and ionic content and was also completed in FY2003. Bulk rock conductivity consists of several components including conduction through fluids in the pore space (electrolytic conduction), surface conduction, and solid matrix conduction (Johnson et al., 1986; Wildenschild et al., 2001). The assessment of changing electrical properties in response to fluid or CO_2 injection requires an understanding of the individual components and this module provides the basis for ascertaining the fluid conduction portion of the bulk conductivity. The remainder of the FY2003 fiscal year was spent developing the appropriate petrophysical models and integration of the laboratory results with the field results.

During the course of fluid injection, sulfide minerals thought to be responsible for significant electrical conduction were not observed after CO_2 injection. Possible causes for the disappearance include solubility in the injection fluid or dissolution due to the formation of carbonic acid because of CO_2 injection. Further study would be required to determine the precise mechanism.

The proposed work includes measurements on additional core samples to further determine the frequency dependence of samples saturated with different fluids and to gain additional information on the changing surface conduction mechanism. Post-sample characterization using geochemical and x-ray imaging methods will help to identify the surface conduction mechanism. We will attempt to use effective medium theory to develop the relationships needed to use the laboratory results to obtain fluid saturation from the field images. One possibility is the use of the lambda parameter, a dynamic length scale, that relates fluid conductivity, permeability, and surface conduction properties

Scanning electron microscope (SEM) (Figure 6) and X-Ray images (Figure 7) show the turbid structure of the diatomaceous ground giving the high porosity and low permeability nature that we are observing in the laboratory and field. These images provide us with an idea of the maximum spatial extent of injected CO_2 into the field. We

estimate over a 15 month period that, not accounting for fracturing and taking into account reservoir pressures, CO_2 flow through the rock matrix should be no more than 15 – 20 meters.

Figure 8 is an example of acquiring an instantaneous snapshot image of the frequency response at different times of core flooding by brine, CO_2, and oil. A core sample in the laboratory apparatus was first saturated with the formation fluid (black line) until the exit fluid was pure formation fluid. Then the core sample was flooded with brine (blue line) until saturated and then CO_2 (red line) until saturated. After these operations, the core sample was swept with a network analyzer from $1.0e^{-4}$ to $5.0\ e^{6}$ Hz at one instantaneous moment. The magnitude (upper) and phase (lower) responses show what differences we should expect in the field at a specified frequency. For example, at 1000 Hz, we would expect to see very little difference in the phase response of oil and CO_2 components, but would expect to see a 20 % increase in amplitude from the magnitude response. This measurement provided us with an expectation of the percent change in electrical resistivity between the oil and CO_2 components.

Figure 9 is a resistivity plot as a function of time for a sample saturated with oil, CO_2, and brine. There is a large difference in the resistivity of the sample when saturated with brine as compared to insulating fluids, but there is also a difference in the electrical properties of the sample saturated by oil and CO_2. The lower plot shows the loss tangent versus frequency for a sample from 482 meters depth, taken from the drilling of the injection well (see Figure 10) with three different pore fluids. The brine-saturated sample has a distinctly different electrical response than the oil or CO_2 saturated samples in the same frequency range as the field data. Frequency dependent measurements highlight the differences and together with multi-frequency field measurements may be the best way to discriminate between fluid phases

The primary conclusion of the laboratory studies is that careful measurements of formation materials with a variety of saturating fluids are necessary for the interpretation of field measurements. Not only do the materials have electrical properties that vary with saturant, but there also exists a time evolution of conduction mechanisms in response to perturbations caused by fluid injection.

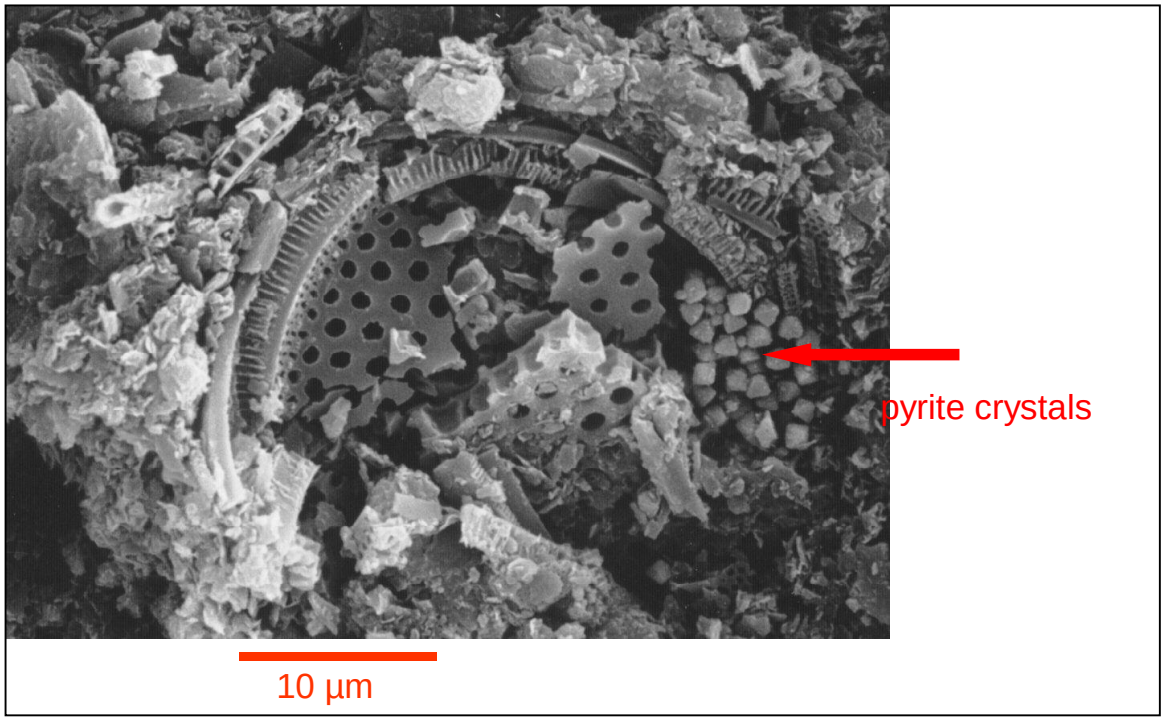

Figure 6: SEM image of the diatomaceous mineral diatomite. The broken structure shows the difficulty of flooding CO_2 and water into a confined geometry. This structure is the reason for an extremely low permeability and high porosity indicative of the CO_2 field used for this LDRD. This image is courtesy of Mike Morea at Chevron-Texaco.

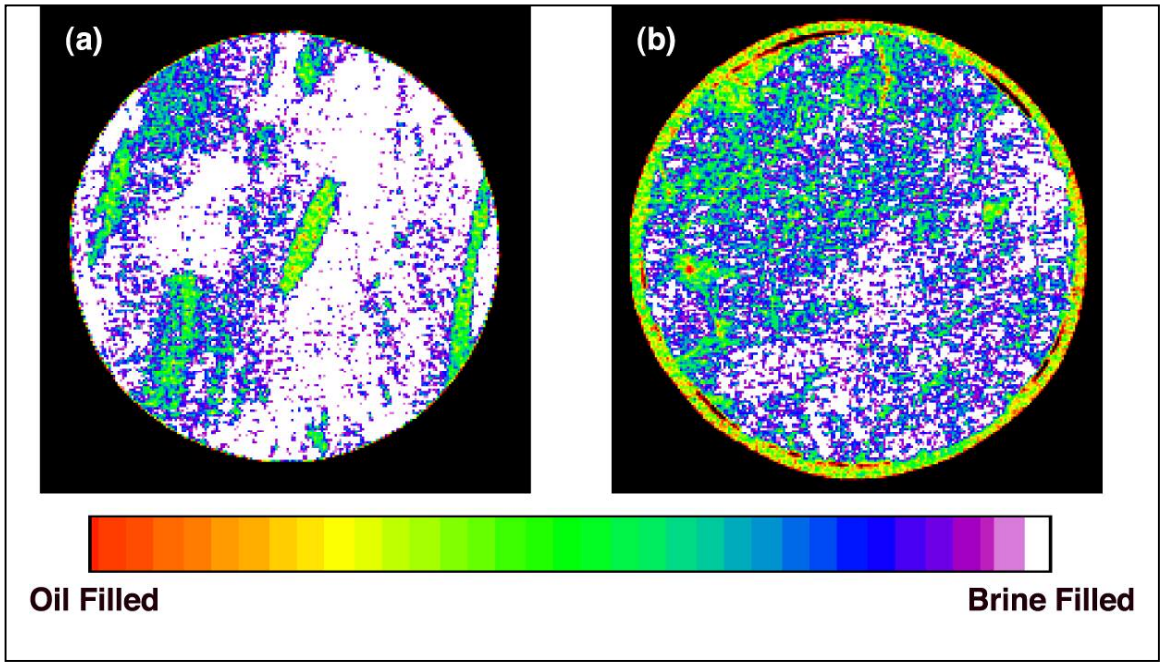

Figure 7: X-ray imaging of core samples before (right image) and after (left image) brine injection. It is clear that pockets of petroleum (green/orange) remain as islands. The significance of this image is in the amount of bypassed petroleum. Therefore, during CO_2 injection, we would expect a large amount of petroleum to become miscible with the CO_2. Further studies will need to consider geochemical analysis of the exit fluid in the laboratory apparatus to determine the volumetric percentage content of CO_2 and petroleum.

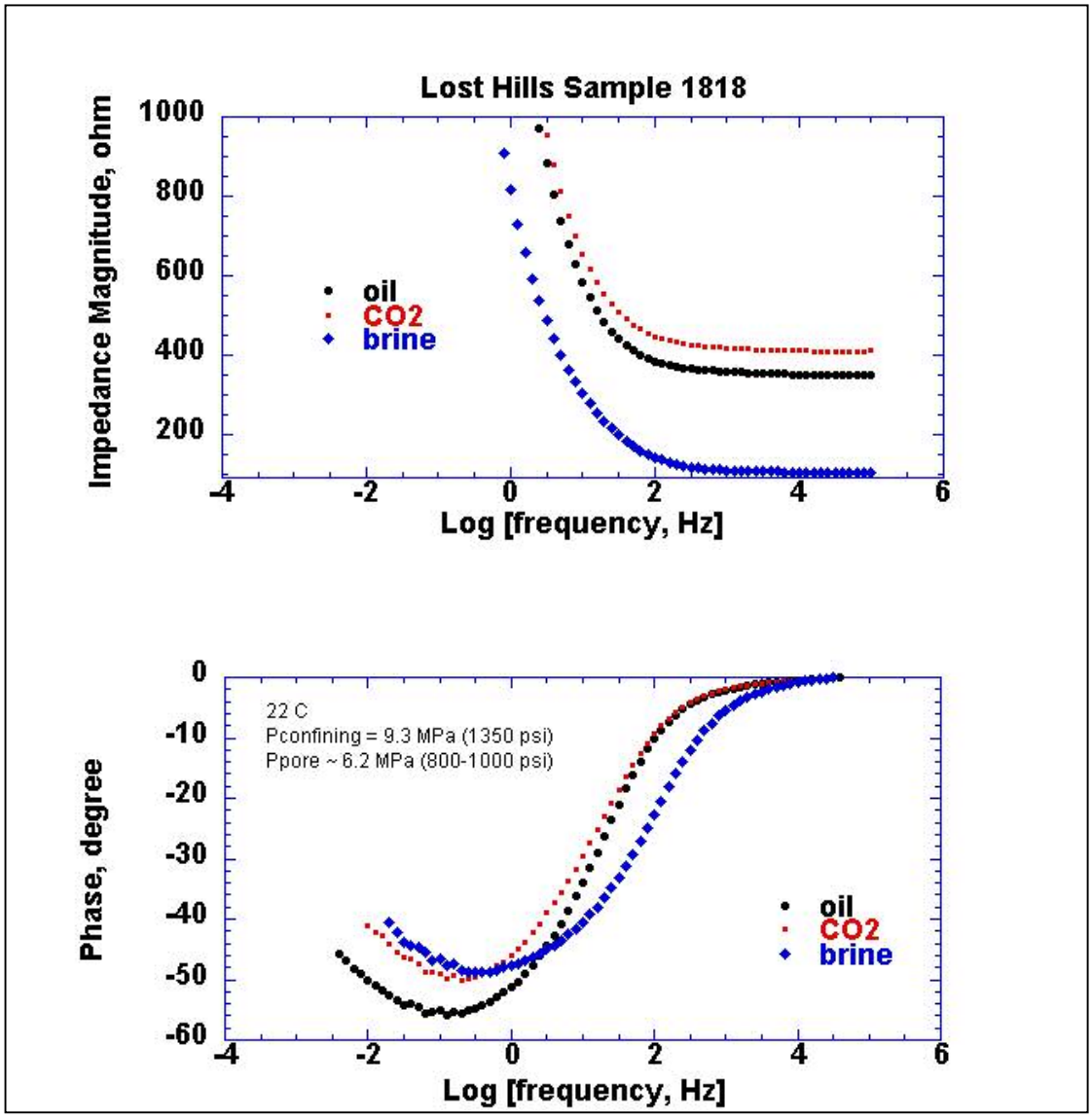

Figure 8: A core sample in the laboratory apparatus was first saturated with the formation fluid (black line) until the exit fluid was pure formation fluid. Then the core sample was flooded with brine (blue line) until saturated and then CO_2 (red line) until saturated. After these operations, the core sample was swept with a network analyzer from $1.0e^{-4}$ to 5.0 e^{6} Hz at one instantaneous moment. The magnitude (upper) and phase (lower) responses show what differences we should expect in the field at a specified frequency. For example, at 1000 Hz, we would expect to see very little difference in the phase response of oil and CO_2 components, but would expect to see a 20 % increase in amplitude from the magnitude response.

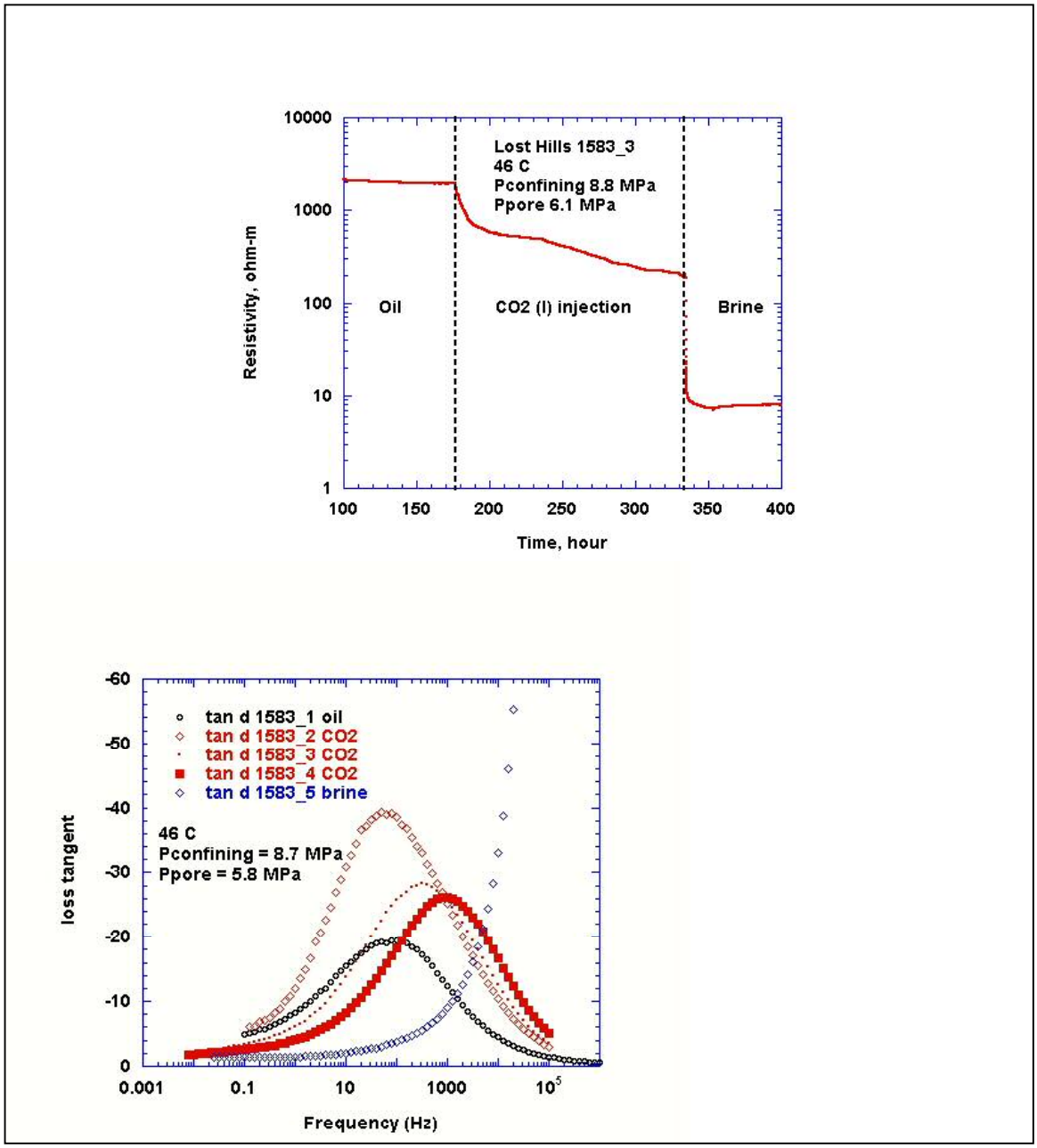

Figure 9: (Upper [a]) Resistivity as a function of time for a sample saturated with oil, CO_2, and brine. There is a large difference in the resistivity of the sample when saturated with brine as compared to insulating fluids, but there is a difference in the electrical properties of the sample saturated by oil and CO_2. (Lower [b]) Loss tangent versus frequency for sample 1583_3 with three different pore fluids. The brine saturated sample has a distinctly different electrical response than the oil or CO_2 saturated samples in the same frequency range as the field data. Frequency dependent measurements highlight the differences and together with multi-frequency field measurements may be the best way to discriminate between fluid phases.

Field Data Techniques

Electromagnetic techniques are sensitive to rock pore fluids within the subsurface, which makes them the ideal method for addressing the problems of enhanced oil recovery (EOR) in a heavy oil environment. In EOR applications, it is also important to discern between injection steam and gases, injection fluids, and formation fluids. The high sensitivity of electromagnetic energy to these physical processes, as well as recent advances in computational ability, inversion code resolution, and field instrumentation, make borehole EM techniques an important tool for such subsurface imaging problems.

During CO_2 sequestration, the high pressure of the injection forces the CO_2 to remain in a liquid or supercritical state. After delivery to the subsurface formation, however, a volume increase can lower pressure causing the CO_2 to a change to the gaseous state. This gaseous state, in addition to other possible liquid and supercritical states, coexists with formation fluid, injection water, and oil. In this complex scenario, EM induction imaging must address the discrimination of fluids and fluid migration in the formation. We know now that this is only possible with laboratory analysis of an individual site – laboratory and field techniques are not separable in this imaging application. Based on initial forward model calculations in addition to processed data sets, we expected, and observed, a large contrast between the formation water and the petroleum / CO_2, but a small contrast between the CO_2 and the petroleum due to the similar inherent electrical conductivities of each component. Resolution of this small contrast necessitates the laboratory experiments and improved processing techniques in order to properly interpret the images.

Figure 3 shows the experimental apparatus to use the crosswell electromagnetic (EM) induction technique to measure the inter-well electrical resistivity or conductivity. The two trucks represent the transmitting antenna and the receiving antenna. Initially, both antennas are lowered into the respective fiberglass observation wells, C1 and C2. The receiving antenna is held fixed while the transmitting antenna, broadcasting a sin wave modulated between 2.0 – 10.0 kHz, is slowly lowered from the top to the bottom of the depth of interest. In this experiment, the depth ranged from 457 – 548 meters, as this was also the depth of CO_2 injection. After the transmitter has completed its run, the receiver is moved 3 meters lower. The well shown in blue in Figure 3 is the injection well for the CO_2 and is the injector well between observation wells C1 and C2 in the lower Figure 1. This pattern is repeated until the receiver reaches the bottom of the depth of interest and repeated further for each frequency, as the nature of EM induction does not allow simultaneous frequencies to be acquired at one time. In this project we focus on frequencies of 2.0, 4.0, 6.0, and 10.0 kHz although this report does not use the 10.0 kHz

datasets as the decreased skin depth of the energy provides too small an imaging window for comparison purposes.

A single frequency data file, which contains all the transmitter and receiver locations, is called a tomography, although this term is not correct in the technical sense. This data is then spatially resampled and splined at discrete points, calibrated to remove the effect of the subsurface on the antenna, formatted to make the data modular, and inverted using a finite difference frequency domain code developed at Sandia National Laboratories. This inversion process requires a starting model that we obtain from the well logs acquired during the drilling process. Further progress has allowed us to use as a starting model the image of the next lowest frequency to decrease the RMS error.

The main impetus of multiple frequency acquisition in this experiment was to allow a more complete response of the CO_2 signature. The frequency-stepping technique mentioned above, as well as the Q-domain approach to spline the frequencies together and invert back to the time domain with a broadband signal, require multiple frequencies. The higher the frequency in EM induction, the higher the interaction with the ground – or the higher the induction number. As the frequency decreases, increased probing depth is obtained at the cost of decreased resolution.

Having acquired low-noise data with new receiver antenna electronics developed in FY2002, we have recently demonstrated that accurate and repeatable data can be acquired at CO_2 sites. Processing and interpretation of the data, therefore, were the primary tasks FY2003. Our overall goal is to provide the basis for qualitative interpretation of the images produced from the field system. The primary technique of achieving this goal is to conduct laboratory measurements of frequency, phase, and amplitude responses of core samples obtained at the site from our corporate sponsor, allowing reasonable limits to be placed on interpretation. Another method requires the development of processing techniques to enhance the small contrast between the oil and the CO_2 response. We can also attempt resolution increases of the images: this is accomplished either in the inversion process with parameter optimizations such as mesh gridding or decreasing the noise in the field data acquisition using techniques to remove the approximation of calibration.

Field Data Results

Field tomographic data was acquired at the site in April, 2001, October, 2001, July, 2002, and October, 2003. In December 2002, well C1 suffered a partial collapse at 300 meters during a logging operation by a Chevron-Texaco contractor and began producing petroleum. This observation well was shutdown as a result. In addition, the CO_2 injection was halted in December 2002 due to issues of the CO_2 degrading the sandpack from the hydraulic fracturing process and causing damage to the producer well pumps.

We examined the feasibility of Q-domain processing. In FY02 we began preliminary work in applying this technique to combine separate images of discrete frequencies into one single image with a finite bandwidth. In FY02, we applied the June, 2002 and October, 2002 data sets, each with three distinct frequencies, to Q-domain analysis. It appears that the Q-domain approach is not an effective solution unless three decades of frequencies in the data are available. Due to the conductive subsurface of the Lost Hills site, resulting in a decreased skin depth, the upper limit of the frequency range is approximately 10 kHz while the lower limit is effectively 1 kHz. While it is possible to conduct EM induction studies at frequencies as low as tens of Hertz, the induction number becomes excessively low and does not allow sufficient interaction between the source field and the CO_2. A more resistive site, such as at the DOE Hanford tank farm, would provide the required three decades of frequency span. Another technique was developed in FY2002 in substitution that used a step-approach to achieve a lower RMS error in the inversion process at subsequently higher frequencies. Essentially, the lower frequencies provide a more accurate starting point for the higher frequency inversions that results in a better fit. This step approach was developed successfully and used in all images displayed in this report.

Figure 10 shows three 4.0 kHz images were acquired at different times: April, 2001 in the upper plot, October, 2001 in the middle plot, and July, 2002 in the lower plot. The green/blue coloring shows the oil and CO_2 mixture while the reddish bar at 507 meters depth and 3.5 Ω-m shows the brine solution being washed away from the west to the east which translates to left to right, in all images displayed in this report. The dotted black line is the approximate position of the injection well and the CO_2/oil is shown to be migrating to the east also with possibly a new CO_2 front being formed below 540 meters depth. The geologic strata are dipping eastward by about 1 – 2 degrees. The reason the CO_2/oil front is broken up is because the CO_2 injection was periodically stopped and brine injection was substituted to keep reservoir pressure up while the CO_2 injection system was cleaned and periodically overhauled.

Figure 11 displays a comparison of multiple frequency images. A 4.0 kHz image on the left and a 6.0 kHz image on the right show very similar features as expected. This data was acquired in October 2001. The higher frequency should provide more resolution of the oil/CO_2 layer shown by the green coloring between depths 520 and 538 meters. The inversion stepping technique was used to decrease the RMS error in the inversion process. For example, the anomaly at 550 meters depth and 7 meters east of the left wells in the 4.0 kHz image is corrected in the 6.0 kHz image. In this manner, we can correct for artifacts caused by a poor starting model.

Figure 12 is a time-lapse set of two-dimensional images of CO_2 flooding in the plane between the two observation wells – one for transmitting, the other for receiving. The left image was generated before injection of CO_2 and after waterflooding, and the center image was generated after five months of injection. The circles on the left side of each image represent the well containing the receiver antenna while those circles on the right side of the images contain the transmitting antenna. The difference image (right) is the pre-injection image subtracted from the during-injection image and shows the areas of change quite clearly. A positive percent difference suggests CO_2 is entering the area at the top left. Blue represents water in place, and yellow and red represent the moving oil and CO_2, respectively. Using laboratory results showing the resistivity values of CO_2, oil, and brine were crucial in delineating between the oil and CO_2, which have similar electrical properties.

We completed the work on optimization of finite difference mesh gridding. We also tested a new technique to remove the process of physical calibration of the field system. Currently, a field system calibration is performed at the end of each day, producing a certain factor that changes from day-to-day based on environmental and system conditions at the time. Temperature is a root factor of these changes as is consistent electrical grounding. In order to remove the calibration process, we are required to develop a method of differencing, or ratioing, adjacent receiver antenna locations and include this in the inversion process. Due to the short two-year term of the LDRD, we were not able to fully implement this method into the inversion as desired, but were able to demonstrate the viability of this technique using the April 2001 4 kHz dataset. One optimized grid for the CO_2 imaging at 4.0 kHz is shown in Figure 13.

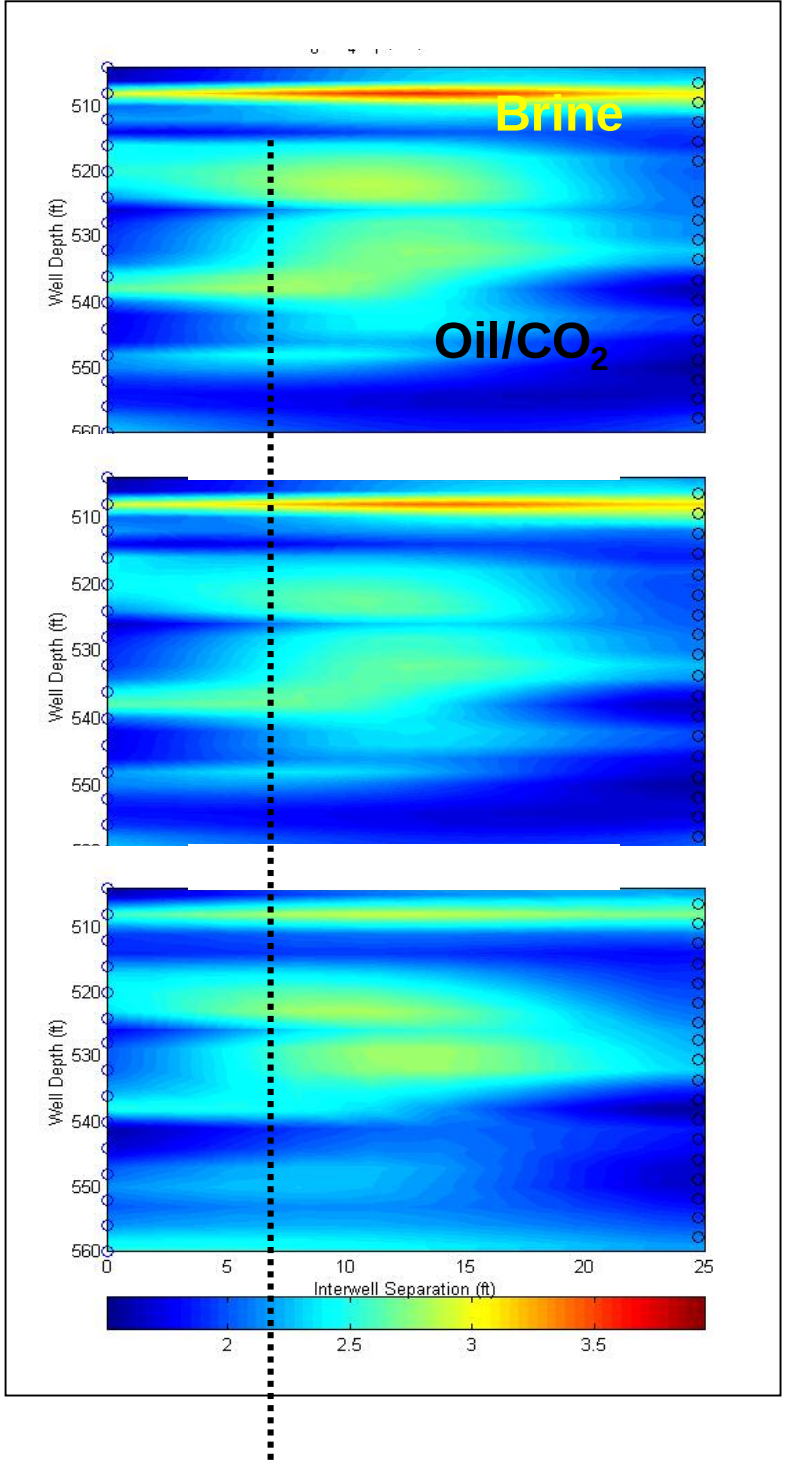

Figure 10: Three 4.0 kHz images were acquired at different times: April, 2001 (upper), October, 2001 (middle), and July, 2002 (lower). The green/blue coloring shows the oil and CO_2 mixture while the reddish bar at 507 meters depth and 3.5 Ω-m shows the brine solution being washed away from the west to the east (left to right, in these images). The dotted black line is the approximate position of the injection well and the CO_2/oil is shown to be migrating to the east also with possibly a new CO_2 front being formed below 540 meters depth. The geologic strata are dipping eastward by about 1 – 2 degrees. The reason the CO_2/oil front is broken up is because the CO_2 was periodically stopped and brine injection was substituted to keep reservoir pressure up while the CO_2 injection system was cleaned and periodically overhauled.

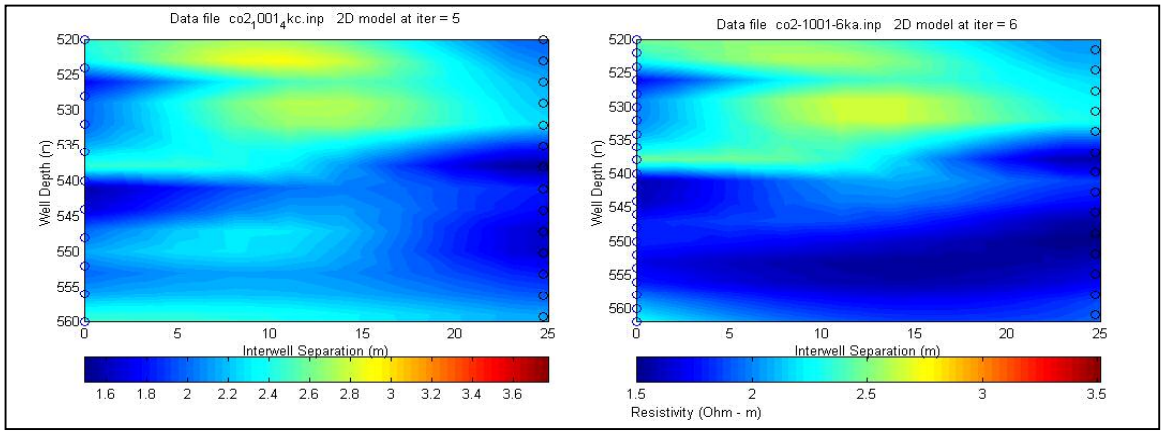

Figure 11: Comparison of multiple frequency images. A 4.0 kHz image (left) and a 6.0 kHz image (right) show very similar features. This data was acquired in October 2001. The higher frequency should provide more resolution of the oil/CO_2 layer shown by the green coloring between depths 520 and 538 meters. The inversion stepping technique was used to decrease the RMS error in the inversion process. For example, the anomaly at 550 meters depth and 7 meters east of the left wells in the 4.0 kHz image is corrected in the 6.0 kHz image. In this manner, we can correct for artifacts caused by a poor starting model.

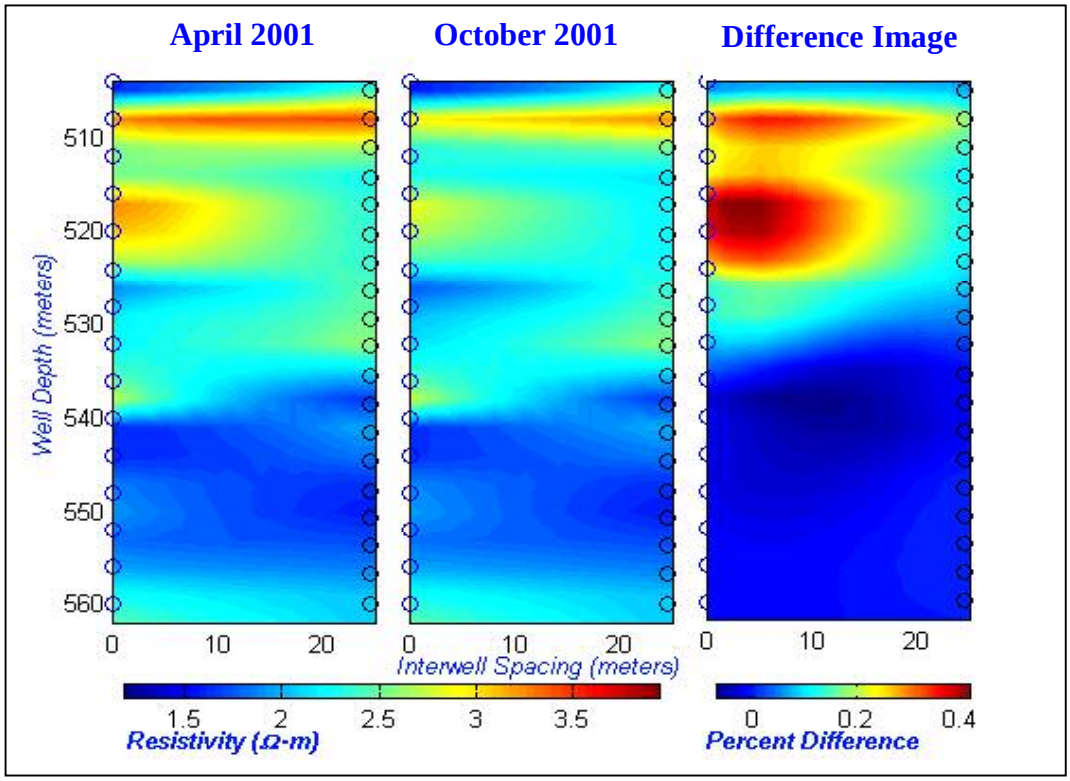

Figure 12: Two-dimensional images of CO_2 flooding in the plane between the two observation wells – one for transmitting, the other for receiving. The left image was generated before injection of CO_2 and after waterflooding, and the center image was generated after five months of injection. The circles on the left side of each image represent the well containing the receiver antenna while those circles on the right side of the images contain the transmitting antenna. The difference image (right) is the pre-injection image subtracted from the during-injection image and shows the areas of change quite clearly. A positive percent difference suggests CO_2 is entering the area at the top left. Blue represents water in place, and yellow and red represent the moving oil and CO_2, respectively. Using laboratory results showing the resistivity values of CO_2, oil, and brine were crucial in delineating between the oil and CO_2, which have similar electrical properties.

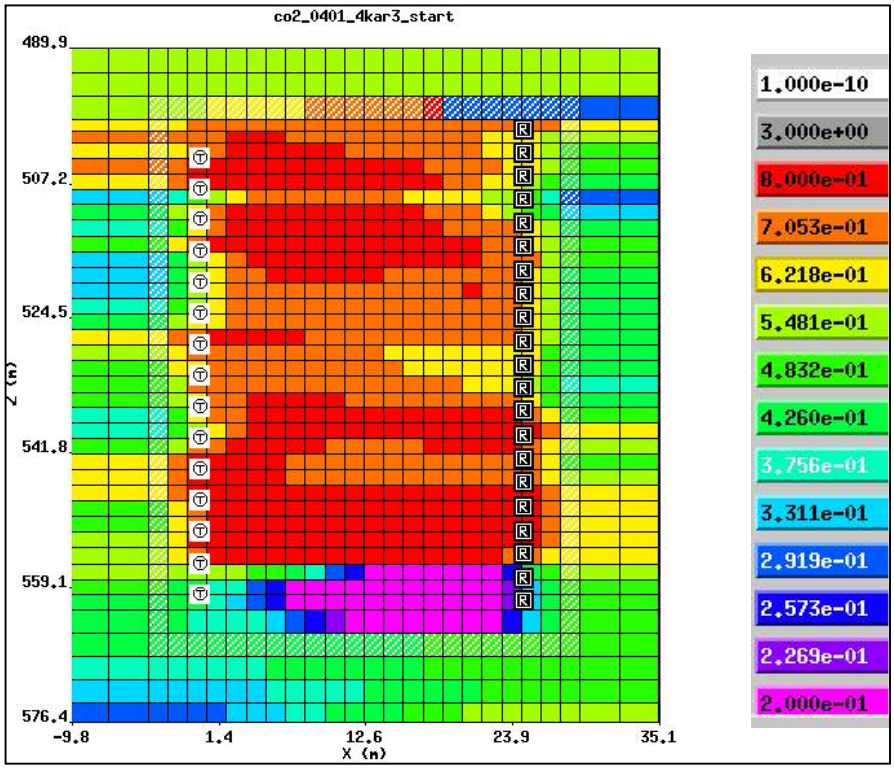

Figure 13: Optimized finite difference grid pattern for site-specific conductivity and source frequency (4.0 kHz). The scale on the right is electrical conductivity (in Siemens/meter). The gridding is actually much larger than shown because the forward model of the inversion code uses reflecting boundaries which can send energy back into the central grid pattern and cause interference. For this reason, we typically extend the grid boundaries to 3 times the skin depth.

Interpretation

One method of discerning between the oil and CO_2 signatures is to look at the resistivity rate of change of the core samples in the laboratory and extrapolate these rates of change to the field images. We refer primarily to the contrast between oil and CO_2. The contrast between brine and CO_2/oil is clear and has been studied and characterized in previous work at LLNL by the authors. The upper plot of Figure 9, for example, shows a characteristic slope in the change of resistivity as a function of time during CO_2 injection. The brine and oil do not display a similar behavior. We determine this CO_2 slope and compare it to the rates of change in Figure 10 which suggest that the CO_2 is moving predominately to the east at a depth interval of 550 – 560 meters and slightly to the west between 540 and 544 meters. The green colored area in Figure 10 is mostly static which likely represents a predominance of oil and is confirmed by well logs acquired during the drilling of the injection well. The slight movement observed in the oil suggests that the CO_2 is affecting the system in the eastern section near a depth of 530 meters. We note that this comparison is only valid for times shortly after CO_2 flooding. In later times, this slope may change or stabilize which would invalidate this rate comparison. One other note to make is that the bottom of these images typically have poor tomographic coverage and have a higher RMS error than areas of better coverage. Therefore, the conductive area at 560 meters depth that appears to be forming may be an artifact of inversion and should not be considered interpretable.

The processing that was developed in this LDRD allows a horizontal resolution of about 2% of well spacing and a vertical resolution of about 0.5 meter, which is a function of the receiver and transmitter antenna length as well as frequency. The Lost Hills site well separation is about 25 meters which places a similar horizontal resolution of about 0.5 meters. Future CO_2 imaging projects with similar oil/ CO_2 contrasts must take into account these limitation to the techniques. Also, frequencies below 1 kHz will not have sufficient resolution to determine effective movement within the time-span of one year in this site and likely less time at other, higher permeability, sites.

Project Results

We have developed a low-noise digital field system to measure the EM induction response to CO_2 in a variety of field conditions. Center to this system is a low-noise induction receiver antenna, which can measure the low-energy response of the CO_2. This system has consistently measured a shallow pseudo-miscible CO_2 flood at source frequencies between 2.0 kHz and 10 kHz. In addition, we have measured the oil and brine also occurring in the formation.

- Comparison with induction logs acquired before drilling suggests the EM induction resolution for CO_2 is equivalent with applications to waterflood imaging.

- We have developed laboratory equipment to conduct fluid and gas time-lapsed injection studies of core samples using fluids acquired in the field. We can measure the resistivity during this process and make instantaneous measurements of the frequency response.

- We have developed an optimum finite difference grid spacing that allows for stable inversions at different frequencies.

- Using time-lapse images, we show the change of electrical conductivity in the field scales to the laboratory results. Using this result, we can approximate an interpretation of field images based on the rate-of-change of the laboratory results.

- We cannot use Q-domain processing unless we have a fairly resistive ground and can use three decades of frequencies. We have access to 2 – 10 kHz data, which is not sufficient to capture the higher frequencies.

- Using these results, we are currently prepared to study other CO_2 sites at greater depths where the CO_2 and existing petroleum components are miscible.

- Journal paper being prepared for submission to Journal of Geophysical International

References

Berryman, J.G., *Analysis of approximate inverses in tomography I. Resolution analysis of common inverses*, Optimization and Engineering, **1**, p.87 – 115 (2000)

Berryman, J.G., *Analysis of approximate inverses in tomography II. Iterative inverses*, Optimization and Engineering, **1**, p.437 – 473 (2000)

Johnson, D.L., J. Koplik, and L.M. Schwartz, 1986, New pore-size parameter characterizing transport in porous media: Phys. Rev. Lett, 57, 2564-2567.

Kirkendall, B.A., Roberts, J.J., 2002, *CO_2 Reservoir Characterization using Electromagnetic Imaging and Controlled Laboratory Experimentation*, 13th Annual Improved Oil Recovery conference, Society of Petroleum Engineers and Department of Energy, Tulsa, Oklahoma, 7 p.

Kirkendall, B.A., Roberts, J.J., 2001, *Electromagnetic Imaging of CO2 Sequestration at an Enhanced Oil Recovery Site*, First National Conference on Carbon Sequestration, Washington D.C., May 14 – 17, 7 p. , UCRL-142753

Wildenschild, D., J. J. Roberts and E. D. Carlberg, Electrical Properties of Sand-Clay Mixtures: The Effect of Microstructure, *Geophys. Res. Lett.*, 27, 3085-3089, 2001.

Wilt, M.J., Lee, K.H., Morrison, H.F., Becker, A., Tseng, H.W., Torres-Verdin, C., Alumbaugh, D., 1995, *Crosswell Electromagnetic Tomography: A New Technology for Oil Field Characterization*, The Leading Edge, SEG, p. 173 – 177

Appendix

Broader Relevance and Future Prospects--Exit Plan

This work is fundamentally scientific in nature, and relevant to continuing DOE Directorate missions in enhanced oil recovery and environmental management. Collaboration with Chevron-Texaco U.S.A. was accomplished on a continual basis sharing data and results as needed. LLNL hosted an on-site meeting with Chevron contacts in February 2002 to display results with Chevron-Texaco. This work had direct application to the currently funded DOE Vision 21 power plant and a proposed NGOTP (Natural Gas and Oil Technology Partnership) proposal for FY04. All technology advances achieved under this study are transferable to that project. This fundamental research is an attempt to improve the understanding of carbon management and carbon dioxide sequestration; issues which will have growing importance in the near future.

The completion of this project allows LLNL to continue a leading role in the development of appropriate field techniques to monitor subsurface processes in the areas of EOR, CO_2 sequestration, and environmental remediation.

Publications and Conferences

Kirkendall, B.A., Roberts, J.J., 2002, *CO_2 Reservoir Characterization using Electromagnetic Imaging and Controlled Laboratory Experimentation*, 75244, 13th Annual Improved Oil Recovery conference, Society of Petroleum Engineers and Department of Energy, Tulsa, Oklahoma, 7 p.

Kirkendall, B.A., Roberts, J.J., 2001, *Electromagnetic Imaging of CO_2 Sequestration at an Enhanced Oil Recovery Site*, First National Conference on Carbon Sequestration, Washington D.C., May 14 – 17, 7 p. , UCRL-142753

Kirkendall, B.A., Roberts, J.J., 2004, *Electromagnetic Imaging of CO2 Sequestration*, Journal of Geophysical International, *In Progress*

Park, S.K., and J.J. Roberts, Conductivity structure of the San Andreas fault, Parkfield, revisited, Geophys. Res. Lett., 30, No. 16, 1842, 2003 UCRL-JC-152099

Park, S K and J.J. Roberts, Conductivity Structure of the San Andreas Fault, Parkfield, Revisited, Eos Trans. AGU, 84(46), Fall Meet. Suppl., Abstract GP12B-03, 2003 UCRL-JC-152099